Journal of Computational and Applied Mathematics 477 (2026) 117196

Contents lists available at ScienceDirect

Journal of Computational and Applied Mathematics

journal homepage: www.elsevier.com/locate/cam

Adapted numerical modeling for fake news diffusion on social networks[☆]

Dajana Conte [a], Samira Iscaro [a], Giovanni Pagano [b],[*], Beatrice Paternoster [a]

[a] Department of Mathematics, University of Salerno, Fisciano, Italy
[b] Department of Agricultural Sciences, University of Naples Federico II, Portici, Italy

ARTICLE INFO

Keywords:
Epidemiological models
Information diffusion
Fake news
ISCR model
Nonstandard finite differences
Elementary stability
Positivity preservation

ABSTRACT

Information diffusion on social media is one of the most critical phenomena of our society that has recently caught researchers' attention, since social media allow users to share any kind of news without, or with very limited, control. In this article, we will focus on a mathematical approach to analyze the spread of fake news on social media. First, we propose a new epidemiological model based on a system of ordinary differential equations of Ignorant–Spreader–Counter Spreader–Recovered (ISCR) type. Secondly, we formulate a Nonstandard Finite Difference (NSFD) scheme for the solution of the problem, that is positivity preserving and elementary stable. The reliability of the proposed model and the efficiency of the derived NSFD method, which will be employed for a phase of parameter estimation using real data, are testified by analyzing the spread of some fake news shared on X in recent years.

1. Introduction

Recent decades have been characterized by the growing popularity of social media, that in just a few years have totally changed our way of approaching everyday life. Our way of buying or selling goods, our political opinions or social events we are involved in, are proofs of how much our life is influenced by social networks. Many people follow the current fashion they see on social media as Instagram or TikTok, or they keep themselves informed using X (Twitter) or other similar social networks. Even several companies try to improve their earnings using e-commerce or personalized advertisement campaigns on social media, trying to enhance these kinds of strategies when the interest towards their products is at maximum level. Equally, during political campaigns, politicians try to persuade people that their programme is the best focusing on topics of interests for the majority of individuals and trying to take advantages from online discussions on those topics.

If on one hand social networks have improved some aspects of everyday life, giving to people the possibility to stay in touch for free and allowing them to know in real time what happens around them, it is certainly true that they have also a role in the process of fake news diffusion.

Therefore, a proper way to analyze the spread of fake news is required. There are several possible approaches to carry out this kind of analysis. They can be based on machine learning techniques, as for example described in [1,2] where machine learning based detectors to discover fake news are presented, or they can be based on mathematical models formulated in terms of differential equations. Certainly, different types of differential equations can be used. Models can be formulated through systems of Ordinary Differential Equations (ODE_S) [3–13], Partial Differential Equations [14], Stochastic Differential Equations [11], or Fractional Differential Equations [15].

☆ This article is part of a Special issue entitled: 'NAMAS-24' published in Journal of Computational and Applied Mathematics.

* Corresponding author.
E-mail addresses: dajconte@unisa.it (D. Conte), siscaro@unisa.it (S. Iscaro), giovanni.pagano5@unina.it (G. Pagano), beapat@unisa.it (B. Paternoster).

https://doi.org/10.1016/j.cam.2025.117196
Received 10 February 2025; Received in revised form 27 September 2025

Available online 7 November 2025
0377-0427/© 2025 The Authors. Published by Elsevier B.V. This is an open access article under the CC BY-NC-ND license (http://creativecommons.org/licenses/by-nc-nd/4.0/).

Among these, one of the most used type of models is represented by the epidemiological ones, i.e., the kind of mathematical models used to describe the evolution of epidemics [16,17]. Epidemiological models are often formulated as systems of ODE$_S$ and are characterized by the fact of being of compartmental type, that means they divide the population in different groups of individuals according to their status, such as susceptible individuals who can be infected, infectious individuals who can transmit the infection, hospitalized, exposed individuals who have been infected but are not infectious yet, recovered, dead, and so on.

Undoubtedly, the number of classes, as well as the number of equations composing the ODE system, are decided in accordance to the characteristics of the epidemic being described. In a similar way, it is possible to proceed with the description of information diffusion on social media. In fact, a news can be compared to a virus: as a virus spreads in a population of living individuals, in a similar way a news spreads in a population of virtual individuals as for example social media users. For this reason, in the following, mathematical epidemiology-like terms will be used while referring to mathematical models for information diffusion, in order to keep the epidemiological interpretation. However, a change of terminology in this particular case is required. According to [5,6,10–12], we recall the following notation:

– *ignorants*, to describe susceptible individuals who can see the news and share it;
– *exposed*, to describe individuals who have read the news, but have not shared anything about it yet;
– *spreaders*, to describe the individuals who share the news and that are the counterpart of infectious individuals present in the description of epidemics;
– *recovered*, to describe the individuals who are no longer interested in sharing the news.

Many other classes can be introduced, according to the main scope of the considered model. Researches in these fields are widespread. For example, in [6,7,18] D'Ambrosio et al. considered a Susceptible–Infected–Recovered (SIR) model and a Susceptible–Exposed–Infected–Recovered (SEIR) model in order to study the spread of fake news on social networks. Such models in the new notation are denoted as Ignorant–Spreader–Recovered (ISR) and Ignorant–Exposed–Spreader–Recovered (IESR), respectively. The authors showed that the parameters of the model can be linked to the ability of a population to recognize fake information and to the grade of access to the Internet, proving, by computing the stiffness ratio of the system (for more details related to the concept of stiffness, see [19, Ch. 7]), that the higher is this quantity the faster a fake news will spread. An interesting formulation of a type of SIR model to analyze information diffusion on social media is also presented in [3,4], where an age group version of this model is proposed to study the impact of users' age in their possible dissemination of a news. More details regarding the age group formulation of epidemiological models can be found in [20].

As previously described, each model is suited to describe a different situation: however, in each case it is fundamental not only to describe the evolution of news spread through time, but also the peak of the maximum spreading both in terms of the moment in time of the peak and in terms of the total number of individuals who share the news. For example, if fake news spread is analyzed, knowing in advance the moment of maximum spreading of the fake information can allow experts to apply countermeasures to block it. Thus, the first goal of this work is to present a new mathematical model to predict the evolution of fake news dissemination on social media. The proposed model, formulated by modifying a model present in literature [11,12], is a multistrain epidemiological model of Ignorant–Spreader–Counter Spreader–Recovered (ISCR) type. This means that it has, along with the two classes of ignorants and recovered, two classes of spreaders and is suitable to describe situations in which a group of individuals (Spreaders) shares a certain fake news while the other group (the Counter Spreaders) tries to restore the truth. Contrary to the model present in [11,12], as explained in the following sections, it also provides the possibility of a non constant population, considering that there are always new subscriptions to a social media and that there can be individuals who, like members of the dead class in epidemiological models, do not contribute to the diffusion process and are removed from each class. Moreover, we prove the positivity of the solution of the new ISCR model and study the stability of the related equilibrium points. Therefore, adapted numerical methods which are able to preserve the above mentioned properties are useful. In the literature, several techniques for deriving stable problem-oriented methods have been studied, see e.g. [21–24]. In particular, starting from techniques used in [8,25–34], the second goal of this work is to develop a Nonstandard Finite Difference (NSFD) scheme that preserves positivity and equilibrium points.

A good parameter estimation phase, also called fitting phase, is fundamental as well, in order to adapt the model to real case studies. According to the used model and to the phenomenon being described, different approaches for the fitting phase can be employed. For example, in [35], Millevoi et al. describe a strategy that provides the use of Physics Informed Neural Networks (PINNs) in order to compute the parameters of a SIR model used to describe the evolution of COVID-19 epidemic, while in [17] the fitting phase to describe the evolution of the same disease is carried out by minimizing the mean square error between real data and approximated ones by exploiting the MATLAB built-in function *lsqnonlin*. In this work, the latter approach with proper modifications will be used, with the aim of obtaining optimized parameters using as less data as possible. That is, we will use only the data corresponding to the initial times of the diffusion of the news for the parameter estimation process. Then, we will show that with the obtained parameters it is possible to accurately predict the peak of diffusion, the related time, and the overall evolution of the news trend, by comparing the solution given by the model with the entire dataset (i.e. also considering the data not used for the fitting phase). Also, as we will see, the use of the newly developed NSFD method will allow to perform the parameter estimation phase with good accuracy despite the choice of non-small discretization step-sizes, at low computing times, thanks both to its good stability properties and to its explicit structure.

The paper will be organized as follows. In Section 2, we describe some models of the literature used to analyze information diffusion. In Section 3 the new ISCR model to analyze the spread of fake news on social networks is presented. We will illustrate some mathematical properties of the model, such as the existence and uniqueness of the solution, its positivity and the stability of

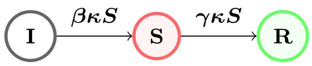

Fig. 1. Graph that shows connections among different classes of the population when the ISR model is used.

the disease free equilibrium point. Section 4 is dedicated to the derivation of the new NSFD scheme with proofs of its positivity and stability with respect to the disease free equilibrium. For simplicity, the other equilibrium points of the continuous and discrete model are reported in the Appendix, and their stability properties are analyzed numerically in Section 5, that is devoted to the experiments. There, tests are carried out on real case studies, since we will describe the evolution of the diffusion of some fake news spread on X in recent years, showing that our model improves the results obtained using models present in literature and confirming at the same time the properties of the proposed nonstandard scheme. Finally, Section 6 is dedicated to concluding remarks and future works.

2. Models for information diffusion

Different mathematical models of epidemiological type have been formulated to describe information diffusion [10–12]. In particular, in [11,12] several models to specifically describe information diffusion on social networks are presented. Among the most useful ones, the following two typologies of models can be considered:

- the *ISR* (Ingorant–Spreader–Recovered) model;
- the *ISCR* (Ignorant–Spreader–Counter Spreader–Recovered) model.

The first typology is the counter part of SIR model for epidemics. Several variations of this model, considering distinct parameter definitions or different interactions among classes of the population, can be formulated. Variants of interest, specific for social networks, are proposed in [11,12].

To formulate the ISR model, the following positive parameters are considered:

- κ, the average number of connections among users of a social network;
- β, the per capita news spreading rate per unit of time, i.e. the parameter that describes the impact of a news spread by each spreader per unit of time. Thus, it rules how fast a news spreads among spreaders, consequently expressing the transition rate from the ignorant class to the spreader class;
- γ, the per capita recovery rate, i.e. the parameter that describes the transition from the spreader class to the recovered class. That is, the outcome of a meeting between two spreaders causes one of the two to lose interest in the news.

Consequently, $\beta\kappa I(t)S(t)$ and $\gamma\kappa S(t)S(t)$ represent the number of effective encounters per unit of time among an ignorant and a spreader and among two spreaders, that lead to the transition of an individual from the ignorant class to the spreader class and from the spreader class to the recovered class, respectively. Moreover, let N be the size of the population, computed as the sum of individuals present in different compartments.

The ISR model reads as follows:

$$\begin{cases} I'(t) = -\beta\kappa I(t)S(t), \\ S'(t) = \beta\kappa I(t)S(t) - \gamma\kappa S(t)S(t), \\ R'(t) = \gamma\kappa S(t)S(t). \end{cases} \tag{2.1}$$

Note that the transition from spreaders to recovered is described by the term $-\gamma\kappa S(t)S(t)$. Following [11,12], it is assumed that spreaders will lose their interest in spreading a news after a confrontation with another spreader (using terminology from mathematical biology, the S-class is ruled by a competition principle). Individuals from other classes do not have influence in the transition from spreaders to recovered: in fact, ignorants have not seen the news yet, while recovered have lost their interest in the news, ending any further contact with other individuals of the population. Observe also that, contrary to the classical SIR for epidemics, the term accounting for recovery is nonlinear. As we will see, this is common in mathematical models for information diffusion. Instead, in the SIR model, this term is linear, being usually of the form $-\gamma I(t)$ (remember that with the SIR–ISR notation change, $I(t)$ in the SIR is the counterpart of $S(t)$ in the ISR).

Fig. 1 represents the dynamics that involves the different populations of the model.

This particular model is suitable to describe a situation in which there is first of all a growth of interest towards a certain news, and then a peak is reached before it vanishes. Several simulations to predict the evolution of some case studies involving both true and fake news using this kind of model have been exhaustively explained in [5]. However, in some cases, it could be required to use a model "ad-hoc" for the description of fake information, in order to better represent the main features of this kind of news. Fake news, for example, can be spread by artificial bots or their diffusion can be encouraged by other means of communication. Moreover, in some cases it could happen that even if a group of users on a social media spreads a certain fake news, another group of users tries to restore the truth by sharing news with an opposite topic. In this cases, traditional models are not sufficient.

Thus, in [11,12], the Ignorant–Spreader–Counter Spreader–Recovered (ISCR) model, to describe this kind of situations, is introduced. To formulate the model the following positive parameters, along with the previous ones already used for the ISR model, are taken in consideration:

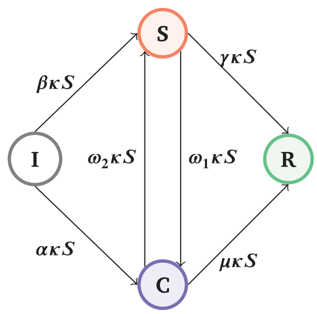

Fig. 2. Graph that shows connections among different classes of the population when the ISCR model [11,12] is used.

– α, the per capita news spreading rate per unit of time among counter spreaders. It is the transition rate from the ignorant class to the counter spreader class;
– μ, the per capita recovery rate for counter spreaders, or equivalently, it rules how fast a news will no longer be of interest among counter spreaders;
– ω_1, the per capita transition rate from spreaders to counter spreaders;
– ω_2, the counter part of the coefficient ω_1, i.e. the per capita transition rate from the counter spreader class to the spreader class.

The $ISCR$ model is formulated as follows:

$$\begin{cases} I'(t) = -\beta\kappa I(t)S(t) - \alpha\kappa I(t)C(t), \\ S'(t) = \beta\kappa I(t)S(t) - (\omega_1 - \omega_2)\kappa S(t)C(t) - \gamma\kappa S(t)[S(t) + R(t)], \\ C'(t) = \alpha\kappa I(t)C(t) + (\omega_1 - \omega_2)\kappa S(t)C(t) - \mu\kappa C(t)[C(t) + R(t)], \\ R'(t) = \gamma\kappa S(t)[S(t) + R(t)] + \mu\kappa C(t)[C(t) + R(t)]. \end{cases} \tag{2.2}$$

A schematic representation of possible interactions among classes in the ISCR model is presented in Fig. 2.

Note that the model (2.2) allows to consider two possible transitions starting from the ignorant class. Contrary to the ISR model previously described, once the user is in the spreader class or in the counter spreader class, there is more than one possibility to exit from the present status. Spreaders can recover, losing interest in the news, going into the recovered class or they can transit into the counter spreader class. Similarly, this situation can happen for counter spreaders. From a mathematical point of view, transitions into the recovered class are described by factors $\gamma\kappa S(t)[S(t)+R(t)]$ and $\mu\kappa C(t)[C(t)+R(t)]$, respectively. These are formulated in this way to take in consideration that spreaders or counter spreaders are influenced in their transition into the recovered class by pre-existing interactions between them and already recovered individuals. Interactions among the two groups of news disseminators are represented by the factor $S(t)C(t)$, multiplied by proper coefficients, that represents virtual encounters of individuals of the two classes. Possible other uses of this model, where different values of parameters are considered, are presented in [11] or [12]. However, this model has some limitations, as highlighted in the following section.

3. A new ISCR model for fake news diffusion

The model (2.2) is suited for the case in which a constant population size is considered, as there are no new entries into or exits from the population. Therefore, it could be used to analyze the spread of news just in a short period of time, considering that, in that time span, there are no other new subscriptions to the considered social media and all users interested by the spread of the analyzed news transit from one class to another. These hypotheses are actually common also in mathematical models for epidemics. Generally, it is assumed that the population is closed. This means that, starting from the initial total population, during the considered period no other individuals can enter and no births or deaths occur.

Although good results can be obtained using these hypotheses, as underlined by numerous works in literature on this topic, it cannot be ignored that during the period of news dissemination, there can be new subscriptions to the considered social media. Thus, new users can enter in the population and interact with groups of spreaders or counter spreaders when the news is already spread and popular. Moreover, during the trending period of a fake news, some users may no longer be able to access the considered social network, for example because they have been blocked since reported as fake profiles or as those spreading fake information, or due to technical problems accessing their accounts during the observation period of the phenomenon.

For these reasons, with the aim of formulating a new model for both the analysis of the dissemination of fake news or of news regarding a high debated topic, we propose a new model of ISCR type, by generalizing the aforementioned one. In particular, we formulate this new ISCR model by adding the following two positive parameters to the classic ISCR (2.2):

– Λ, which represents the new add rate to the ignorant class. It can be seen as the number of the new subscriptions to the social media, or as the number of new individuals who enter in the population, per unit of time, i.e. the number of the new

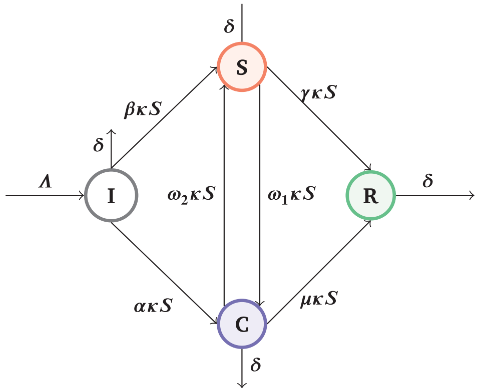

Fig. 3. Graph that shows connections among different classes of the population when the ISCR model of (3.1) is considered.

individuals per unit of time that start to be interested in the news because they have heard about it due to external influences as television, oral confrontations, newspapers and so on and that now can encounter in a virtual way other individuals that are sharing contents regarding it;

- δ, representing the per capita death rate. Note that there may be individuals who have been blocked because they were reported as fake profiles, or who could not access the social network for technical reasons during the considered observation period. Consequently, these individuals represented by the quantities $\delta I(t)$, $\delta S(t)$, $\delta C(t)$, $\delta R(t)$ are removed from the corresponding class.

Considering the motivations behind required changes, we can formulate the new model as follows in (3.1), considering that the factor Λ can be introduced in the first equation of (2.2) since newcomers are still in an ignorant state:

$$\begin{cases} I'(t) = \Lambda - \beta\kappa I(t)S(t) - \alpha\kappa I(t)C(t) - \delta I(t), \\ S'(t) = \beta\kappa I(t)S(t) - (\omega_1 - \omega_2)\kappa S(t)C(t) - \gamma\kappa S(t)[S(t)+C(t)] - \delta S(t), \\ C'(t) = \alpha\kappa I(t)C(t) + (\omega_1 - \omega_2)\kappa S(t)C(t) - \mu\kappa C(t)[S(t)+C(t)] - \delta C(t), \\ R'(t) = \gamma\kappa S(t)[S(t)+C(t)] + \mu\kappa C(t)[S(t)+C(t)] - \delta R(t). \end{cases} \tag{3.1}$$

Fig. 3 shows a graph to illustrate the relationships among different classes.

Focusing on the new model, another remark is required. In fact, the changes compared to the classic ISCR are not limited to the definition of the new parameters, but have also been performed in the second and third equations. Transitions to the recovered class, contrary to the ISCR model present in literature, are formulated as $\gamma\kappa S(t)[S(t)+C(t)]$ and $\mu\kappa C(t)[S(t)+C(t)]$, respectively. The change is due to the meaning we are giving to the recovered class. Since recovered are individuals no longer interested in supporting one or another group of spreaders, it is reasonable to assume that they will no longer share anything related to the news being analyzed. Thus, individuals from the spreader or counter spreader class will not lose their interest in sharing a news because of their relationships with people of recovered class, simply because these encounters are not possible due to the fact that recovered do not share anything anymore. The loss of interest can be motivated by a debate between individuals of the two classes. For example, spreaders or counter spreaders, after a debate with the opposite class, can be convinced that their opinion is the right one, losing their interest in a further possible dissemination of their ideas, transiting into the recovered compartment. As a consequence, also the equation for $R(t)$ has been modified. Other important modification affects the size of the population N, that is as follows:

$$N(t) = I(t) + S(t) + C(t) + R(t). \tag{3.2}$$

Observe that, in model (2.2), as common in literature, $N'(t) = 0$ meaning that the total population size is constant. However, this does not apply to the new ISCR model, since newcomer individuals are being considered, as well as the possibility of exit from the different classes at rate δ. Indeed, considering (3.1), population evolution through time is not constant but described by the simplified logistic equation (for more details regarding this particular equation, see [16])

$$N'(t) = \Lambda - \delta N(t). \tag{3.3}$$

Before presenting numerical methods to solve the new introduced model, and before describing the model validation process, it is important to explore some of its analytical properties. In the following, we will show that the solution of the Cauchy problem related to (3.1) exists, it is unique, and non-negative if the initial conditions are non-negative. Furthermore, we will prove that all the non-negative solutions of (3.1) are ultimately bounded. Equilibrium points of the system will be analyzed as well, investigating at the same time some relevant quantities such as reproduction numbers (for more details on these quantities, see for example [36,37]). In this section, we also analytically analyze the stability of the disease free equilibrium. As regards the stability of the other equilibrium points, that can be derived and studied in a similar way, an analysis will be numerically carried out in Section 5, on some real case studies.

Remark 1. From now on we will suppose that $\omega_1 \geq \omega_2$. When we analyze fake information, this choice is motivated by the following reasoning. The parameter ω_1 indicates the transition rate from the spreader class to the counter spreader class. It can be interpreted as the possibility that spreaders are convinced that the news they are spreading is false and thus, by passing into the counter spreader class, they will try to restore the truth. Moreover, as explained in [2,7], fake information spreads faster than true one. Therefore, it is more likely that, when a fake news is shared, spreaders are more than counter spreaders. For this reason, it is also more likely a transition towards the counter spreader class than contrary situation.

3.1. Positivity and uniqueness of the solution

In this section, we will explore some mathematical properties of the solution.

Theorem 1. *For each choice of the initial condition, the solution of the Cauchy problem related to the model (3.1) locally exists and is unique.*

Proof. The model (3.1) can be written as

$$Y'(t) = F(Y(t)),$$

where $Y = \left[I(t), S(t), C(t), R(t)\right]^T \in \mathbb{R}^4$ and $F : \mathbb{R}^4 \to \mathbb{R}^4$, with

$$F(Y) = -\delta Y + B(Y), \qquad B(Y) = \begin{bmatrix} \Lambda - \beta\kappa IS - \alpha\kappa IC \\ \beta\kappa IS - (\omega_1 - \omega_2)\kappa SC - \gamma\kappa S[S+C] \\ \alpha\kappa IC + (\omega_1 - \omega_2)\kappa SC - \mu\kappa C[S+C] \\ \gamma\kappa S[S+C] + \mu\kappa C[S+C] \end{bmatrix}. \tag{3.4}$$

The proof of local existence and uniqueness of the solution follows by observing that each component of F is a polynomial ($F \in C^\infty(\mathbb{R}^4)$). Therefore, F is locally Lipschitz continuous. Thus, we get the thesis by the Picard–Lindelöf theorem (see [19, Th. 1.3]). $\square$

From now on, let us denote $I_0 = I(0),\ S_0 = S(0),\ C_0 = C(0),\ R_0 = R(0)$.

Theorem 2. *If $I_0,\ S_0,\ C_0,\ R_0 \geq 0$, then the solution of the Cauchy problem related to (3.1) is non-negative $\forall t \geq 0$. Moreover, if the initial conditions are positive, then the solutions of the corresponding Cauchy problem are positive $\forall t \geq 0$.*

Proof. The proof is done following a strategy similar to that used in [4]. Without loss of generality, we will focus on the case in which the initial conditions are positive.

Let us consider the first equation of the model (3.1). From it we get

$$I'(t) + I(t)(\beta\kappa S(t) + \alpha\kappa C(t) + \delta) = \Lambda > 0. \tag{3.5}$$

By defining

$$a(t) = \exp\left(\int_0^t (\beta\kappa S(h) + \alpha\kappa C(h) + \delta)dh\right),$$

from (3.5), multiplying its terms for $a(t)$, it follows

$$\frac{d}{dt}[I(t)a(t)] = I'(t)a(t) + I(t)(\beta\kappa S(t) + \alpha\kappa C(t) + \delta)a(t) > 0.$$

Therefore, $I(t)a(t)$ is an increasing function, and we have

$$\forall t \geq 0, \quad I(t)a(t) > I_0 a(0),$$

$$I(t)\exp\left(\int_0^t (\beta\kappa S(h) + \alpha\kappa C(h) + \delta)dh\right) > I_0.$$

Since by hypothesis $I_0 > 0$ then

$$I(t) > I_0 \exp\left(-\int_0^t (\beta\kappa S(h) + \alpha\kappa C(h) + \delta)dh\right) > 0.$$

By proceeding similarly for the second equation, we get

$$\frac{d}{dt}[S(t)b(t)] = 0,$$

with

$$b(t) = \exp\left(\int_0^t -(\beta\kappa I(h) - (\omega_1 - \omega_2)\kappa C(h) - \gamma\kappa(S(h) + C(h)) - \delta)dh\right).$$

Then, $S(t)b(t)$ is constant. Since $b(0) = e^0 = 1$ and $S_0 > 0$ by hypothesis, we have

$$\forall t \geq 0, \quad S(t)b(t) = S_0 b(0),$$
$$S(t) = \frac{S_0}{b(t)} > 0.$$

Similarly, from the third equation, we get

$$\frac{d}{dt}[C(t)d(t)] = 0,$$

with

$$d(t) = \exp\left(\int_0^t -(\alpha\kappa I(h) + (\omega_1 - \omega_2)\kappa S(h) - \mu\kappa(S(h) + C(h)) - \delta)dh\right).$$

Therefore, since $d(0) = e^0 = 1$ and $C_0 > 0$ by hypothesis, we have

$$\forall t \geq 0, \quad C(t)d(t) = C_0 d(0),$$
$$C(t) = \frac{C_0}{d(t)} > 0.$$

From the fourth equation, since by previous proofs $S(t)$ and $C(t)$ are positive $\forall t \geq 0$, we have

$$\frac{d}{dt}[R(t)g(t)] > 0,$$

with

$$g(t) = \exp\left(\int_0^t (\delta R(h))dh\right).$$

$R(t)g(t)$ is a strictly increasing function. Since $g(0) = e^0 = 1$ and $R_0 > 0$ by hypothesis, we have

$$\forall t \geq 0 \quad R(t)g(t) > R_0 g(0),$$
$$R(t) > R_0 \exp\left(-\int_0^t (\delta R(h))dh\right) > 0.$$

This concludes the proof of the theorem. □

Remark 2. Note that, from (3.3), the total population reads as

$$N(t) = e^{-\delta t}\left(N_0 - \frac{\Lambda}{\delta}\right) + \frac{\Lambda}{\delta},$$

where N_0 is a given initial condition for the size of the total population ($N_0 = I_0 + S_0 + C_0 + R_0$). Therefore, there exists $L > 0$ such that $N(t) \leq L, \forall t > 0$, and so, considering also Theorem 2 and (3.2), we have

$$0 \leq I(t), S(t), C(t), R(t) \leq L, \quad \forall t > 0.$$

Thus, we conclude that the solution of the Cauchy problem related to model (3.1) is bounded.

From Theorem 1 and Remark 2, note that the solutions of the Cauchy problem related to (3.1) are globally defined.

3.2. Equilibrium points

In this subsection, emphasis will be given to the analysis of the equilibrium points of the new ISCR model in (3.1). Since the ISCR model is a multistrain epidemiological model, four types of points are expected [16]. In particular, solving $F(Y) = 0$, with F as in (3.4), leads to the following equilibrium points:

- the *Disease Free Equilibrium* (*DFE*), that is obtained when both $S(t) = 0$ and $C(t) = 0$. It is the point
$$\{I_{DFE}, S_{DFE}, C_{DFE}, R_{DFE}\} = \left\{\frac{\Lambda}{\delta}, 0, 0, 0\right\}; \tag{3.6}$$
- the *Spreader Prevalence Equilibrium* (*SPE*), that is obtained when $C(t) = 0$, and describes the situation in which spreaders are dominant. Its expression is reported in Appendix;
- the *Counter spreader Prevalence Equilibrium* (*CPE*), that is obtained when $S(t) = 0$, and describes the situation in which counter spreaders are dominant. Its expression is reported in Appendix;
- the *Coexistence Equilibrium* (*CE*), that is obtained when $S(t) \neq 0$ and $C(t) \neq 0$, and describes the situation in which there is no dominance of spreaders over counter spreaders and vice versa. It is reported in Appendix.

The asymptotic stability properties of the equilibrium points are studied by evaluating the eigenvalues of the Jacobian matrix in correspondence of them, as explained below. From now on, let us indicate with $\Re(\lambda)$ the real part of λ, with $\lambda \in \mathbb{C}$. Moreover, below we consider the definition of asymptotic stability in the sense of Lyapunov.

Theorem 3. *[38, Ch. 4, p. 268] An equilibrium point for a system of ODE_S is locally asymptotically stable if the real part of all the eigenvalues of the Jacobian matrix, evaluated in correspondence of this point, is less then 0. Furthermore, it is unstable if there exists at least one eigenvalue λ of the Jacobian matrix such that $\Re(\lambda) > 0$.*

In this subsection, we focus on the analysis of the DFE, which, as known, can be used to infer various insights about the dynamics of an epidemic. For example, if the DFE is asymptotically stable, one can expect the epidemic to die out under initial conditions sufficiently close to it. Similarly, in the context of fake information spreading, this would indicate that, after an initial phase of diffusion, the news will gradually lose popularity, eventually leading to a complete loss of interest among social network users. By analyzing the DFE, it is also possible to derive reproduction numbers, that is, using terminology from mathematical epidemiology, the number of second infections due to the presence of a spreader or a counter spreader, respectively. Actually, since the ISCR model is a multistrain epidemiological model with two classes of infectious, two different reproduction numbers can be derived, as well as an overall reproduction number that describes if the epidemic will spread or not. The last one, in particular, is the maximum between the previous two values [16].

The Jacobian matrix of the system (3.1) evaluated at the DFE reads

$$J = \begin{bmatrix} -\delta & -\frac{\beta\kappa\Lambda}{\delta} & -\frac{\alpha\kappa\Lambda}{\delta} & 0 \\ 0 & -\delta + \frac{\beta\kappa\Lambda}{\delta} & 0 & 0 \\ 0 & 0 & -\delta + \frac{\alpha\kappa\Lambda}{\delta} & 0 \\ 0 & 0 & 0 & -\delta \end{bmatrix},$$

whose eigenvalues are

$$\lambda_1 = -\delta, \quad \lambda_2 = -\delta, \quad \lambda_3 = -\delta + \frac{\alpha\kappa\Lambda}{\delta}, \quad \lambda_4 = -\delta + \frac{\beta\kappa\Lambda}{\delta}. \tag{3.7}$$

According to [16, p. 185] we have that the reproduction numbers associated to the spreader and counter spreader classes are respectively given by

$$R_1 = \frac{\beta\kappa\Lambda}{\delta^2} \quad \text{and} \quad R_2 = \frac{\alpha\kappa\Lambda}{\delta^2}. \tag{3.8}$$

Then, the stability properties of the DFE are given in Theorem 4 below.

Theorem 4. *The disease free equilibrium of the new ISCR model in (3.1) is locally asymptotically stable if $R_1 < 1$ and $R_2 < 1$. If $R_1 > 1$ or $R_2 > 1$, it is unstable.*

Proof. The DFE is asymptotically stable if all eigenvalues of J are less than zero. Since $\delta > 0$, then the eigenvalues λ_1 and λ_2 in (3.7) satisfy this property. Consider now λ_3 and λ_4 in (3.7). Then

$$-\delta + \frac{\beta\kappa\Lambda}{\delta} < 0 \Rightarrow R_1 = \frac{\beta\kappa\Lambda}{\delta^2} < 1,$$

and

$$-\delta + \frac{\alpha\kappa\Lambda}{\delta} < 0 \Rightarrow R_2 = \frac{\alpha\kappa\Lambda}{\delta^2} < 1.$$

This concludes the proof. □

4. A NonStandard finite difference method for the proposed model

In Section 3, a new ISCR model to describe fake news diffusion on social networks was presented and some of its analytical features were described as well. In order to apply it for the analysis of real case studies, a proper numerical method is also required. Indeed, as we will see in the next section, to describe the spread of information extracted from a social network, we need to optimize the model parameters by minimizing the mean squared error between the available real data and the solution obtained by solving the ODE system. This parameter optimization phase requires solving the ODE model several times, and the use of standard methods may not be efficient. By the way, explicit methods may suffer from instability issues, while implicit methods may be excessively expensive since they require the solution of systems of nonlinear equations at each time step. For these reasons, exploiting the so-called NonStandard Finite Differences (NSFD), we propose in this section a new method with computational cost similar to the one of explicit methods. However, compared to standard explicit methods, this NSFD method will be proved to be stable. In addition, we will construct it in order to preserve the positivity and the properties of the equilibrium points of the exact solution for each choice of step-size. Similarly to Section 3 for the continuous case, also for the discrete model we here analyze the stability of the disease free equilibrium. The stability of the other equilibrium points will be investigated numerically in Section 5 for some real case studies.

Firstly introduced by Mickens [34,39,40], NSFD methods have had a great impact on literature regarding numerical methods to solve epidemiological models, since by following some construction rules they can be positivity preserving and have good stability properties. These rules are described e.g. in [25–28,30,34], and briefly recalled below. Consider an ODE problem of the form

$$\begin{cases} y'(t) = f(t, y), \\ y(t_0) = y_0, \end{cases} \quad \text{with} \quad t \in [t_0, t_{end}], \tag{4.1}$$

with $f : [t_0, t_{end}] \times \mathbb{R}^m \to \mathbb{R}^m$ and $y : [t_0, t_{end}] \to \mathbb{R}^m$. Let $\{t_n | t_n = t_0 + nh, n = 0 \dots N, t_N = t_{end}\}$ be a discretization of the time interval.

Consider a Standard Finite Difference (SFD) scheme for (4.1). In our case, we consider the explicit Euler method. Starting from it, a nonstandard method can be obtained by considering:

- an approximation of the following type of the derivatives of y,

$$y'(t_n) \approx \frac{y_{n+1} - \Psi(h) y_n}{\Phi(h)},$$

  being $y_n \approx y(t_n)$, where the functions $\Psi(h)$ and $\Phi(h)$ are non negative functions called *numerator function* and *denominator function*, respectively, satisfying, for $h \to 0$,

$$\Psi(h) = 1 + \mathcal{O}(h) \quad \text{and} \quad \Phi(h) = h + \mathcal{O}(h^2).$$

  Note that for $\Psi(h) = 1$ and $\Phi(h) = h$ we recover a standard approximation of the derivative;
- a non local approximation of nonlinear terms in $f(t, y)$ involved into the problem. For example, if $f(t, y) = y^2$, we can consider $y^2(t_n) \approx y_{n+1} y_n$.

As shown below and discussed e.g. in [26], the above rules, appropriately adapted to the continuous problem under consideration, can be used to modify a selected standard explicit method; in our case we consider the explicit Euler method as starting scheme. The starting method should be modified so that it remains explicit and also preserves important properties of the continuous solution, such as positivity and stability of the equilibrium points. Let us note that the application of the above rules does not affect the order of convergence of the Euler method, which is equal to one, since they introduce an $\mathcal{O}(h)$ perturbation to it. These rules can also be generalized to the case of numerical methods with higher order than Euler, see e.g. [26, Def. 5].

In view of the stability properties of method, we recall the following definition from [25].

Definition 1. A numerical scheme is called elementary stable whenever it has no other fixed points than those of the continuous system it approximates, and the local stability of these fixed points is the same for both the discrete and the continuous dynamical systems for each value of the step-size h.

Consider now the ISCR model proposed in (3.1). By taking into account the previous rules, we formulate the following nonstandard finite difference scheme for its solution:

$$\begin{cases} \frac{I_{n+1}-I_n}{\Phi(h)} = \Lambda - \beta\kappa I_{n+1} S_n - \alpha\kappa I_{n+1} C_n - \delta I_n, \\ \frac{S_{n+1}-S_n}{\Phi(h)} = \beta\kappa I_{n+1} S_n - (\omega_1 - \omega_2)\kappa S_{n+1} C_n - \gamma\kappa S_{n+1}(S_n + C_n) - \delta S_n, \\ \frac{C_{n+1}-C_n}{\Phi(h)} = \alpha\kappa I_{n+1} C_n + (\omega_1 - \omega_2)\kappa S_{n+1} C_n - \mu\kappa C_{n+1}(S_n + C_n) - \delta C_n, \\ \frac{R_{n+1}-R_n}{\Phi(h)} = \gamma\kappa S_{n+1}(S_n + C_n) + \mu\kappa C_{n+1}(S_n + C_n) - \delta R_n. \end{cases} \tag{4.2}$$

Equivalently, (4.2) can be rewritten as follows:

$$\begin{cases} I_{n+1} = \frac{(1-\delta\Phi(h))I_n + \Lambda\Phi(h)}{1+\beta\kappa\Phi(h)S_n + \alpha\kappa\Phi(h)C_n}, \\ S_{n+1} = \frac{(1-\delta\Phi(h)+\beta\kappa\Phi(h)I_{n+1})S_n}{1+(\omega_1-\omega_2)\kappa\Phi(h)C_n + \gamma\kappa\Phi(h)(S_n+C_n)}, \\ C_{n+1} = \frac{(1-\delta\Phi(h)+\alpha\kappa\Phi(h)I_{n+1}+(\omega_1-\omega_2)\kappa\Phi(h)S_{n+1})C_n}{1+\mu\kappa\Phi(h)(S_n+C_n)}, \\ R_{n+1} = (1-\delta\Phi(h))R_n + \Phi(h)(\kappa(\gamma S_{n+1} + \mu C_{n+1}))(S_n + C_n). \end{cases} \tag{4.3}$$

Let us define

$$N_n = I_n + S_n + C_n + R_n, \qquad \forall n \geq 0. \tag{4.4}$$

Then, we can formulate the following theorem, which states that the law related to the total population of the continuous model is preserved by the discrete scheme.

Theorem 5. *N_n in (4.4) is an approximation of order 1 of $N(t_n)$ in (3.2).*

Proof. By adding the terms of the equations in (4.2) or (4.3), we get

$$N_{n+1} = N_n + \Phi(h)\Lambda - \delta\Phi(h)N_n,$$

or equivalently

$$\frac{N_{n+1} - N_n}{\Phi(h)} = \Lambda - \delta N_n.$$

Since $\Phi(h) = h + \mathcal{O}(h)$, in view of (3.3), it holds true that $N_n = N(t_n) + \mathcal{O}(h)$. $\square$

Note that, by construction, the method (4.3) has trivially order of convergence equal to one. Depending on the denominator function under consideration, a different NSFD scheme can be obtained from (4.2) or (4.3). Our main aim is to choose a denominator function such that the numerical scheme is positive and elementary stable, i.e. such that it preserves the equilibrium points of the continuous model and their stability properties. To achieve this goal, the following denominator function is considered:

$$\Phi(h) = \frac{1-e^{-\delta h}}{\delta}. \tag{4.5}$$

Theorem 6. *The NSFD scheme proposed in (4.2) or (4.3) is positive* $\forall h > 0$ *if the denominator function in (4.5) is used.*

Proof. Observe that, since $\omega_1 \geq \omega_2$ from Remark 1, by induction, using positive values of I_0, S_0, C_0, R_0, the solution provided by the NSFD method (4.3) is positive if the quantity $1 - \delta\Phi(h)$ present in each equation is positive.

In particular, using the denominator function defined in (4.5), we have

$$1 - \delta\Phi(h) = 1 - \delta\frac{1-e^{-\delta h}}{\delta} = e^{-\delta h} > 0 \quad \forall h > 0.$$

Therefore, the proof follows. □

As already mentioned, another important property that can be achieved by properly constructing a nonstandard method is elementary stability. That is, the requirement that the equilibrium points of the continuous model and their asymptotic properties are preserved in the discrete case for each $h > 0$. It can be shown that, for the new ISCR (3.1), the equilibrium points of the NSFD method (4.3) correspond to those of the continuous model, as explained in Appendix. Furthermore, using the denominator function (4.5), we show below that the asymptotic behavior of the DFE, i.e. the equilibrium point obtained when both spreaders and counter spreaders are zero (see Section 3.2), is the same both for the continuous model and for the discrete method. As for the other points, in Section 5 we will show that their asymptotic equilibrium properties are preserved by the numerical method for at least some values of the model parameters.

Theorem 7. *[16, Th. 16.3]. An equilibrium point for a discrete-time system is locally asymptotically stable if the magnitude of all the eigenvalues of the related Jacobian matrix, evaluated in correspondence of this point, is less than 1. Furthermore, it is unstable if there exists at least one eigenvalue of the Jacobian matrix that has magnitude greater than 1.*

Theorem 8. *The stability properties of the DFE (3.6) are preserved by the NSFD scheme (4.3)* $\forall h > 0$. *This means that, in view of Theorem 4, for the discrete system, the point is locally asymptotically stable if* R_1 *and* R_2 *in (3.8) satisfy* $R_1 < 1$ *and* $R_2 < 1$. *Furthermore, it is unstable if* $R_1 > 1$ *or* $R_2 > 1$.

Proof. In order to study stability properties of the DFE, by considering conditions highlighted in Theorem 7, we compute the spectrum of the Jacobian matrix of the system in (4.3) and evaluate it in correspondence of this point, obtaining the following eigenvalues:

$$\lambda_1 = 1 - \delta\Phi(h), \quad \lambda_2 = 1 - \delta\Phi(h), \quad \lambda_3 = 1 - \delta\Phi(h) + \frac{\beta\kappa\Lambda\Phi(h)}{\delta}, \quad \lambda_4 = 1 - \delta\Phi(h) + \frac{\alpha\kappa\Lambda\Phi(h)}{\delta}.$$

Note that $|\lambda_1| = |\lambda_2| < 1\ \forall h > 0$. In fact, $\Phi(h) = \frac{1-e^{-\delta h}}{\delta}$ and $1 - \delta\Phi(h) = e^{-\delta h} > 0\ \forall h > 0$. Moreover, since $\delta > 0$ and $e^{-\delta h} > 0$ $\forall h > 0$, then $1 - \delta\Phi(h) < 1$.

Focus now on the other two eigenvalues. Observe that, since $\delta\Phi(h) = 1 - e^{-\delta h} < 1\ \forall h > 0$, then $\delta\Phi(h) < 2$ or equivalently $\delta < \frac{2}{\Phi(h)}$. Thus $|\lambda_3| < 1$ and $|\lambda_4| < 1$ if and only if the following relations hold:

$$\begin{cases} \frac{-2\delta+\delta^2\Phi(h)}{\kappa\Lambda\Phi(h)} < \beta < \frac{\delta^2}{\kappa\Lambda}, \\ 0 < \alpha < \frac{\delta^2}{\kappa\Lambda}. \end{cases} \tag{4.6}$$

Consider the first condition of (4.6). Note that, since $\delta\Phi(h) < 2$, then

$$-2\delta + \delta^2\Phi(h) < -2\delta + 2\delta = 0.$$

The quantity $\frac{-2\delta+\delta^2\Phi(h)}{\kappa\Lambda\Phi(h)} < 0\ \forall h > 0$. It is always true that $\beta > 0 > \frac{-2\delta+\delta^2\Phi(h)}{\kappa\Lambda\Phi(h)}$. Thus, by considering the relations in (3.8), note that the first equation of (4.6) is satisfied when $R_1 < 1$, while the last condition reads $0 < R_2 < 1$. Furthermore, from the above computations, it also follows that, if $R_1 > 1$ or $R_2 > 0$, then $|\lambda_3| > 1$ or $|\lambda_4| > 1$, respectively. This concludes the proof. □

5. Numerical experiments

In this section, we illustrate the reliability of the new ISCR model proposed in (3.1) for the description of the evolution of the spread of some fake news shared on the social network X in recent years. Simulations will be carried out by solving the problem with the NSFD scheme proposed in (4.3), showing its advantages in comparison to other numerical schemes from the literature. Furthermore, we show that using an appropriate strategy to obtain optimized parameters from real data, it is possible to make predictions on the spread of news. In our numerical tests, we will consider datasets of real data: we optimize the parameters of

Table 1
Technical details on the used datasets.

Hashtag/Event	Date (dd-mm-yyyy)	Observation period	Available tweets	Type
#DCBlackout	01-06-2020	2 days	33 117	Fake
#Spiderman4	04-04-2022	10 h	7341	Fake
#SarahPalin	01-08-2009	33 h	4677	Fake
#mahsaamini	24-09-2022	30 h	3000	True

the models using a small amount of data, exploiting the remaining available ones to verify the accuracy of the made predictions. In particular, datasets of real data are built using two tools, namely the *Twitter Developer Option* [41] and the Python data scraper *Tweepy* [42], to extract data from X (Twitter), and the algorithm described in [5] to organize them in such a way that they can be used for our aims.

To perform the parameter estimation phase, we minimize the mean square error between some of the available real data and the estimated ones, obtained through the considered model. The parameter optimization process is performed exploiting the MATLAB *lsqnonlin* function, using the same settings described in [5], but with appropriate modifications based on the used model. Once the fitting phase has been carried out, with the obtained parameters and the considered model it is possible to predict the evolution of the news spread. In particular, it is important to take into account the time of its maximum diffusion and the corresponding number of spreaders. To compute optimized parameters, *lsqnonlin* solves a nonlinear least squares problem: starting from an initial approximation of the parameters, it determines them by minimizing a chosen function. In our case, we select the function to be minimized as the sum of the squared errors between real data and computed ones, on spreaders and recovered:

$$f(\text{par}) = \sum_{n=1}^{\tilde{n}} (S_n - S_{\text{true}}(t_n))^2 + \sum_{n=1}^{\tilde{n}} (R_n - R_{\text{true}}(t_n))^2.$$

Here: $\tilde{n}$ is the number of data used for the prediction phase; S_n and R_n are the approximated number of spreaders and recovered at time t_n; $S_{\text{true}}(t_n)$ and $R_{\text{true}}(t_n)$, taken from the dataset, are the corresponding true total number of individuals which are spreaders and removed at time t_n; par is a vector containing all the free parameters to be estimated. Since the *lsqnonlin* function involves a trust-region method based on an iterative process, it solves several times the considered ODE model, until it finds the final set of parameters. As we will see from numerical experiments, the use of the NSFD method that we have constructed in Section 4 allows to efficiently perform the parameter estimation phase.

Since the new ISCR model is primarily aimed at analyzing the spread of false information, the case studies under consideration are mainly related to the diffusion of fake news on X. However, as described above, this model is very versatile, being also suitable to describe the spread of information that is not necessarily fake. Indeed, it describes situations where two opposite groups of spreaders are involved, and is able to analyze the evolution of news related to highly debated topics. For this reason, in numerical experiments we also analyze a true news. Specifically, we will consider the evolution of the treads of the following hashtags, and consequently the evolution of news linked to them.

– *#DCBlackout* [10]: fake news related to possible problems with communications in Washington D.C. due to the Black Lives Matter movement.
– *#Spiderman4* [5]: fake news related to a possible release of a new film of Spiderman trilogy of movies with actor Tobey Maguire.
– *#SarahPalin* [9]: fake news spread in 2009 regarding a possible divorce of Governor of Alaska, Sarah Palin.
– *#mahsaamini* [43]: true news related to the death of Mahsa Amini. She was a Kurdish woman arrested by Iranian police on September 2022 because accused of wearing in a wrong way the hijab, violating Iranian laws. Forced to undergo to a "re-education" programme, she was interned into a detention center where a violent beating caused her a cerebral hemorrhage that let to her death.

Technical details on datasets related to each news are reported in Table 1.

5.1. Validation of the model and parameters estimation

The goal of this subsection is to show that the new ISCR model proposed in this work improves the predictions on news diffusion obtained with some other models from the scientific literature introduced for this purpose. By the motivations expressed in [5], to predict the spread of the news previously presented, we involve in the optimization process related to the new ISCR model (3.1) the parameters β, α, γ, μ, κ_0, ω_1, ω_2. The only parameters not considered for the estimation phase are the rate Λ used for the ignorant class and the mortality rate δ. Indeed, we set $\Lambda = 0.00023$ and $\delta = 0.001$. In particular, Λ has been chosen in this way according to a parameter with a similar meaning employed in [6], where the authors analyze the dissemination of fake information in several countries, using different datasets and obtaining good results in all cases. Regarding δ, we suppose that the number of individuals that cannot access to their account during the observation period is quite small. Therefore, the value for δ has been fixed in such a way that it is at least of one order of magnitude lower than the parameters that describe the transition from a class to another involved into the model. As already mentioned, in this subsection we compare the new ISCR model with two models from the literature for the dissemination of information on the web, both able to describe the evolution of true or false news. Specifically,

Table 2
Optimal parameters for the new ISCR model.

Hashtag	β	α	γ	μ	κ_0	ω_1	ω_2
#DCBlackout	0.3	0.03	0.30001	0.04	0.2	1.6581	1.0589
#Spiderman4	0.20438	0.1	0.30001	3.5	0.2	1.2279	0.94123
#SarahPalin	1.5	0.07	0.03	0.04	0.02	3.5	0.02
#mahsaamini	0.1	0.1	0.1	0.3	0.29993	0.5	0.4

Table 3
Predictions of the time at which the peak of the news spread occurs, by the new ISCR model (for which we used the NSFD method (4.3) with $h = 2$), the ISR and the reference ISCR models (for which we used the MATLAB routine *ode45*). We refer to: t_p as the actual time of the peak; t_p^* as the estimated time of the peak; Err_{t_p} as the relative error on t_p.

		New ISCR		ISR		ISCR	
Hashtag	t_p	t_p^*	Err_{t_p}	t_p^*	Err_{t_p}	t_p^*	Err_{t_p}
#DCBlackout	160	161	0.00625	157.28	0.0170	133.52	0.16550
#Spiderman4	151	123	0.18543	106.11	0.29731	92.778	0.38558
#SarahPalin	371	329	0.11321	278.11	0.25039	285.07	0.23161
#mahsaamini	191	211	0.10471	137.85	0.27826	167.52	0.12296

we compare the new ISCR with the ISR and the classic ISCR models [11,12], whose formulation is recalled in (2.1) and (2.2), respectively. For all these three models, we consider $\kappa = \frac{\kappa_0}{N_0}$, being $\kappa_0 > 0$ and N_0 the total number of individuals of the population at initial time. This is done to take into account the fact that the average total number of connections between individuals during the diffusion of a given news item is influenced by the size of the population (we use N_0 as an indicator of the latter).

In numerical tests, for the solution of the new ISCR model, which is performed several times during the parameter estimation process, we employ the adapted nonstandard finite difference scheme (4.3) proposed in Section 4. Note that the ODE model derived to describe the spread of fake news clearly provides an approximation of the actual data trend. That is, even by solving the ODE model requiring increasingly greater accuracy from the numerical method, the error with respect to the (exact) real data does not fall below a certain threshold (given by the difference between the data observed in reality and the solution of the ODE model, regardless of the numerical method used for it). Therefore, decreasing the discretization step-size does not necessarily guarantee an improvement in errors compared to real data. On the contrary, since the model has to be solved repeatedly during the parameter optimization process, it is preferable to use discretization steps that are quite large for efficiency reasons. This is possible if the numerical method has good stability properties, which is the case of the new proposed NSFD scheme. Indeed, as shown below, choosing $h = 2$ leads to good results, e.g. comparable with those obtained by the MATLAB routine *ode45* in terms of error, and better in terms of computing times. As for the other two models ISR and classic ISCR, as done in [5], we use the MATLAB routine *ode45*.

The optimal parameters for the considered news, obtained with the new ISCR model, are reported in Table 2. Moreover, Figs. 4 and 5 show the predictions made by the three considered models for the respective optimal parameter values. In these figures, the data denoted with * (in green) have been used for the fitting phase, while the remaining data denoted with • (in red) are reported just to check the accuracy of the predictions obtained with the used models. For each news, in the parameter estimation phase, we have considered from 25 to 60 data, according to the related features, see also [5]. From Figs. 4 and 5 note that, in comparison to the ISR and to the classic ISCR, the new ISCR model is able to better predict both the maximum number of spreaders and the time corresponding to the peak of the spread. To visualize this aspect in detail, we report in Tables 3 and 4 the relative errors by the three models associated to these quantities. That is, these tables show respectively the errors related to: the actual time of the peak of the news dissemination (i.e. the time corresponding to the maximum number of spreaders), the actual value of the peak (i.e. the maximum number of spreaders).

As can be observed, the new ISCR model produces better results than the ISR model and the ISCR reference model, both for fake and true news. In particular, the ISR model fails to accurately predict the evolution of news such as #SarahPalin, since the peak is underestimated, or #Spiderman4 and #mahsaamini, since the peak is overestimated. For these latter news, the results obtained are also far from the real data. Instead, the classic ISCR model performs better than ISR, but still does not accurately predict the peak for all the considered news (it is often anticipated), nor does it faithfully describe the overall trend of the news. Both of these aspects are better accounted for by the new ISCR model. Moreover, by comparing the values of the errors reported in Tables 3 and 4 obtained using the three analyzed models for all the news, it can be seen that the performances in the case of the #DCBlackout are in general better than the others. This is due to the features of the used dataset. In fact, for #DCBlackout, the data are characterized by good regularity, with little significant fluctuations, particularly at the time points used during the fitting phase. On the contrary, the data relating to the other news show more pronounced oscillations, as visible in Figs. 4 and 5.

5.2. Advantages of the NSFD scheme

In this subsection, we show the efficiency of the proposed NSFD method (4.3), which we have proved to be unconditionally positive and stable. In particular, we show that the new NSFD method permits to conduct the phase of estimation of parameters with

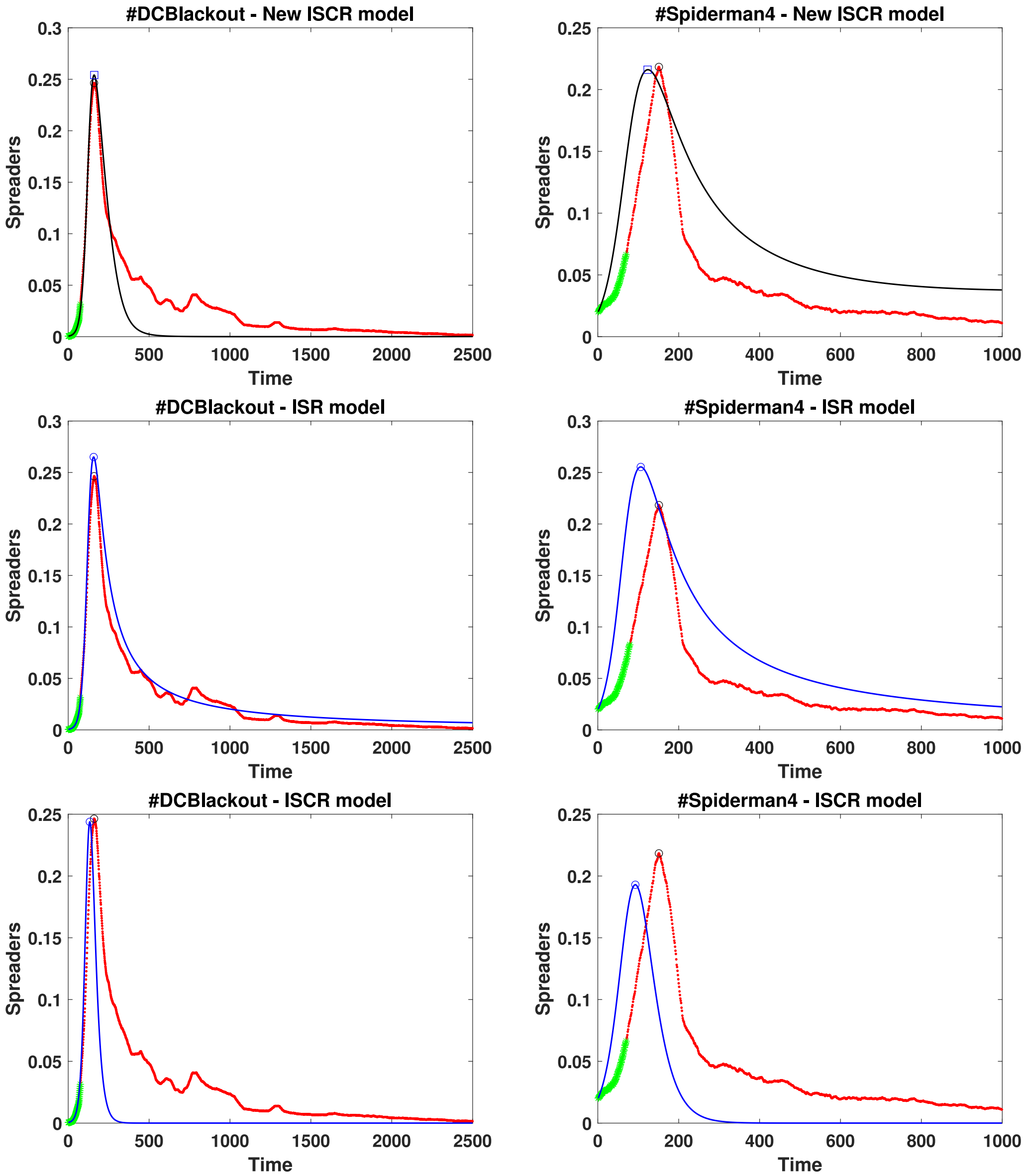

Fig. 4. Prediction of news spread using the new ISCR model, the ISR model, and the classic ISCR model for #DCblackout (on the left) and #Spiderman4 (on the right). *: data for the fitting phase. •: data for prediction. -: solution of the model.

Table 4
Predictions of the maximum number of spreaders by the new ISCR model (for which we used the NSFD method (4.3) with $h = 2$), the ISR and the reference ISCR models (for which we used the MATLAB routine *ode45*). We refer to: S_p as the true maximum number of spreaders; S_p^* as the estimated maximum number of spreaders; Err_{S_p} as the relative error on S_p.

		New ISCR		ISR		ISCR	
Hashtag	S_p	S_p^*	Err_{S_p}	S_p^*	Err_{S_p}	S_p^*	Err_{S_p}
#DCBlackout	0.246	0.254	0.03143	0.265	0.0758	0.244	0.01009
#Spiderman4	0.218	0.216	0.01022	0.255	0.1700	0.193	0.11632
#SarahPalin	0.220	0.207	0.06010	0.182	0.1755	0.257	0.16752
#mahsaamini	0.247	0.241	0.02520	0.759	2.0696	0.232	0.06020

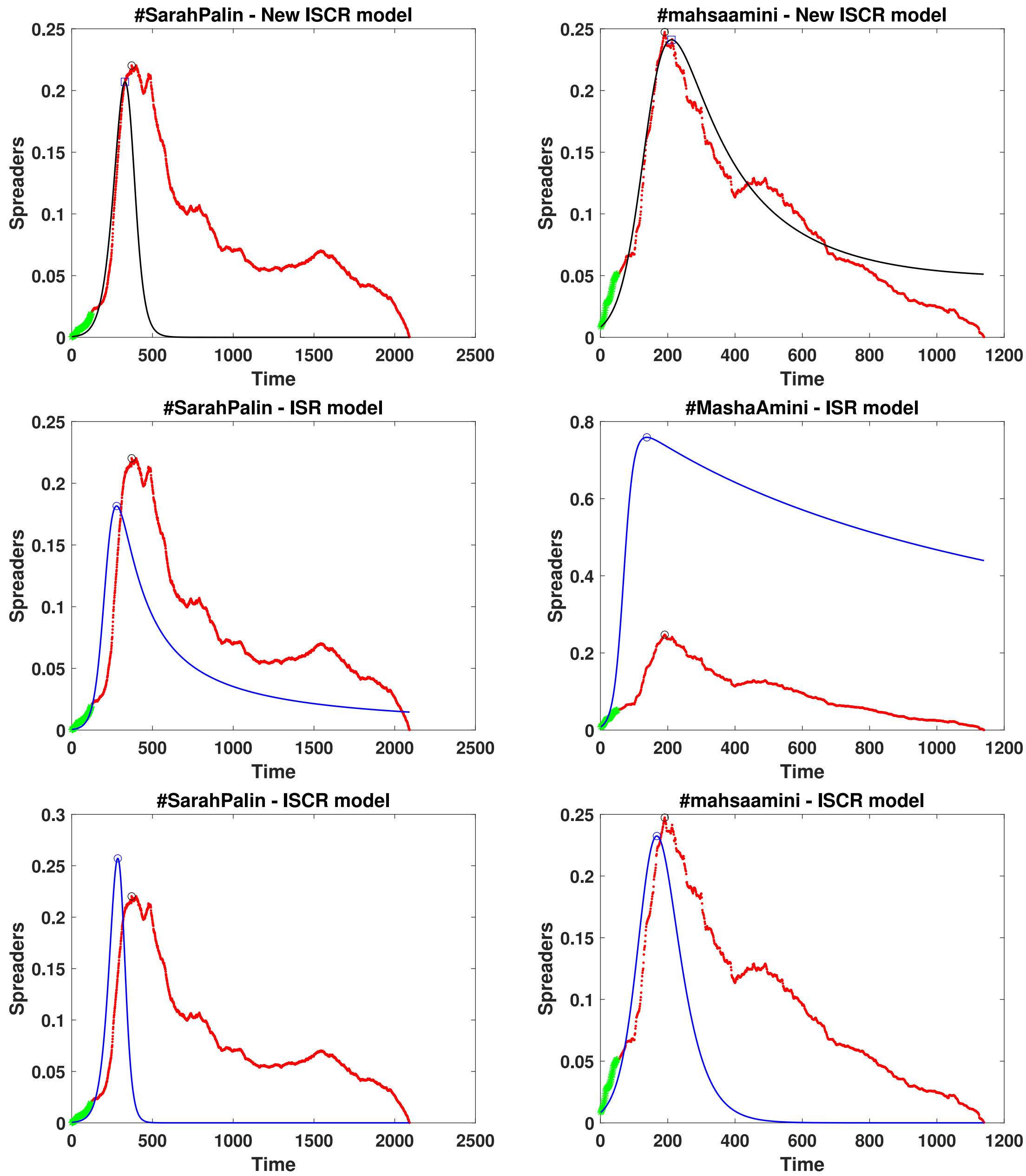

Fig. 5. Prediction of news spread using the new ISCR model, the ISR model, and the classic ISCR model for #SarahPalin (on the left) and #mahsaamini (on the right). *:data for the fitting phase. •: data for prediction. -: solution of the model.

good accuracy, stability and employing lower computing times than other standard methods. Also, here we confirm the elementary stability of the NSFD method.

First of all, we experimentally verify the order of convergence of the developed NSFD scheme (4.3) by considering the parameters in Table 2 for #DCBlackout, $t \in [0, 1000]$, through the formula

$$p_{\text{est}} = \frac{\log(\text{err}(2h)) - \log(\text{err}(h))}{\log(2)}.$$

Here, $\text{err}(h)$ is the relative error in 2-norm computed by considering the solution at all grid points, by the NSFD scheme with step size h, with respect to a reference solution obtained via the MATLAB routine *ode45*, that has been applied by requiring maximum accuracy. The experimental order of convergence obtained in this way is reported in Table 5. Note that, in order to compute it using the formula written above, we have solved the problem by progressively halving the step-size value, starting from $h = 0.1$.

Table 5
Estimated order of convergence by the NSFD scheme (4.3).

Time step-size h	p_{est}
0.1	–
$\frac{0.1}{2}$	0.9967
$\frac{0.1}{2^2}$	0.9984
$\frac{0.1}{2^3}$	0.9992
$\frac{0.1}{2^4}$	0.9996
$\frac{0.1}{2^5}$	0.9998
$\frac{0.1}{2^6}$	0.9999
$\frac{0.1}{2^7}$	0.9999
$\frac{0.1}{2^8}$	1.0000
$\frac{0.1}{2^9}$	1.0000

Table 6
Relative errors on the time of the peak and on the maximum number of spreaders, and employed CPU time for the parameter estimation process, on the #DCBlackout news with the new ISCR model.

	Method	Err_{t_p}	Err_{S_p}	CPU time
$h = 2$	NSFD scheme (4.3)	0.01	0.0305	1.438
$h = 2$	Implicit Euler	0.08	0.0425	37.58
tol $= 10^{-3}$	*ode45*	0.05	0.0514	6.688

Let us now compare the new NSFD scheme with the implicit Euler method, which also has order one, and with the MATLAB routine *ode45*, on the new ISCR model. The comparisons have been performed by using these methods for the parameter estimation phase on the #DCBlackout news. In accordance with the previous subsection, we have used $h = 2$ for the NSFD scheme, and also for the implicit Euler method. We mention that we have considered for comparison also the explicit Euler method with the same time step-size $h = 2$. However, it suffers from instability issues and is unable to provide any result. For this reason, we do not report results due to its use. Moreover, we have applied *ode45* with relative tolerance 10^{-3}. In this way, the used methods lead to errors of the same order of magnitude.

The results are reported in Table 6, where we show the relative errors on the time of the peak and on the total number of spreaders obtained with the estimated parameters. In the table we also report the CPU time employed by the methods for the parameter estimation phase. From the results, note that the NSFD scheme is advantageous as it provides relatively low errors and with less CPU time than all other used numerical methods. Actually, the implicit Euler method takes long computing times as it requires the solution of a nonlinear system of equations at each time-step. On the other hand, the Matlab routine *ode45* provides comparable errors with respect to those obtained using the NSFD method, but employing higher computing times than it. Therefore, having a stable method able to provide reliable solutions even for large step-sizes is useful, especially for problems like the ones addressed in this paper where it is necessary to solve the considered differential equations model several times to perform a phase of estimation of the related parameters. This highlights the advantages of the new NSFD method proposed in this paper.

As mentioned in Section 4, the NSFD method is capable of preserving the positivity of the solution and also the equilibrium points of the new ISCR model and their properties. In particular, in Sections 3 and 4, respectively, we proved that the DFE is an equilibrium point of the continuous model and is preserved by the discrete method. The other equilibrium points of the continuous model are reported in the Appendix. Using the *Mathematica* software, we have checked that the NSFD method (4.3) has the same equilibrium points.

Below, we numerically show the elementary stability of the NSFD method for all considered news. That is, using the parameters in Table 2, we computed the equilibrium points and the related asymptotic stability properties for both the new ISCR model (3.1) and the NSFD method (4.2) or (4.3), verifying that they correspond in the continuous and discrete cases. The results are reported in Table 7, that shows the stability properties of all equilibria for the considered news. Here, the symbol "-" denotes the unacceptability of the associated equilibrium point for the used parameters.

Finally, Figs. 6 and 7 confirm the theoretical results proved for the DFE point. Indeed, recall that this point is stable if $R_1 = \frac{\beta\kappa\Lambda}{\delta^2} < 1$ and $R_2 = \frac{\alpha\kappa\Lambda}{\delta^2} < 1$, and unstable otherwise. Thus, on the #DCBlackout news, i.e. with the parameters of the first row in Table 2, the DFE point is unstable, as also shown in Table 7. Using a slight perturbation of the initial condition corresponding to the DFE, this is indeed confirmed in Fig. 6, where it can be observed that the solution is asymptotically far from equilibrium. Instead, by using parameters for which $R_1 < 1$ and $R_2 < 1$, note that the solution returns to the initial state, even by perturbing the initial condition corresponding to the equilibrium, as shown in Fig. 7.

Table 7
Stability of the equilibrium points for the new ISCR model on the considered news, both in the continuous and discrete case.

Point	#DCBlackout	#Spiderman4	#SarahPalin	#mahsaamini
DFE	Unstable	Unstable	Unstable	Unstable
SPE	Unstable	Stable	Unstable	Stable
CPE	Unstable	Unstable	–	Unstable
CE	Stable	–	Stable	–

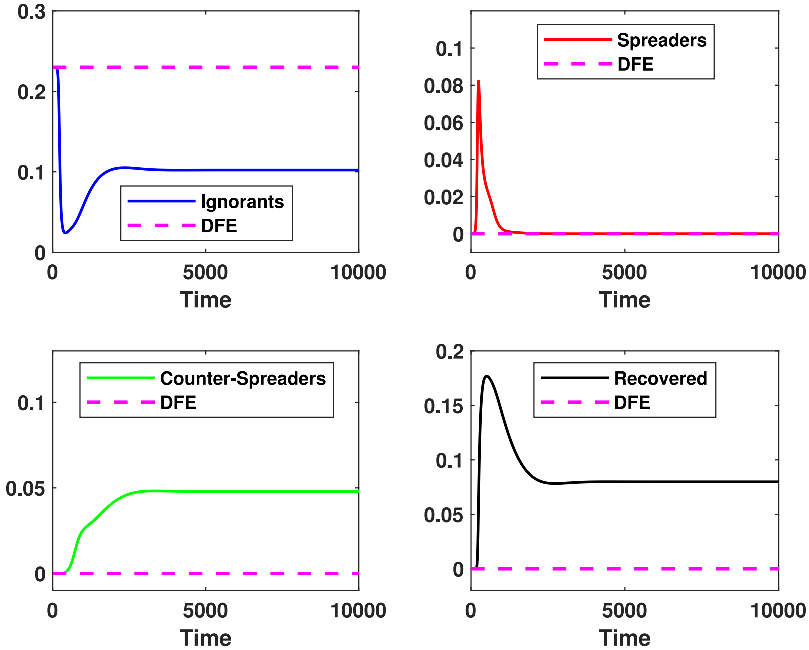

Fig. 6. Numerical solution of the new ISCR with the NSFD method (4.3) for $h = 2$, considering the parameters related to the #DCBlackout news in Table 2, and as initial condition $I_0 = \frac{\Lambda}{\delta}$, $S_0 = C_0 = R_0 = 0.000001$.

6. Conclusions and future research

In this work, a new epidemiological model of Ignorant–Spreader–Counter Spreader–Recovered type for the study of the spread of fake information on social media was presented. We have analyzed important properties of the new model, such as positivity, equilibrium points and related stability properties. Moreover, a numerical method based on nonstandard finite differences for its solution was introduced, able to preserve all the main properties of the continuous model for each value of the step-size. Finally, through several numerical experiments, we have shown the efficiency of the new nonstandard method for the parameter estimation phase and highlighted that the proposed ISCR model can actually be used to describe the spread of high debated true or fake news, improving the models present in the literature for these purposes.

Future research can concern the development of other adapted numerical methods to further improve the efficiency of the parameter estimation phase. Furthermore, it would be interesting to investigate the behavior of the newly proposed ISCR model for the analysis of other news involving a large number of data.

It would also be worthwhile to further investigate a more general formulation of the proposed model, in which some key parameters, such as Λ, are functions depending on the total population size. In this case, however, the overall dynamics of the system are not necessarily guaranteed to coincide with those previously obtained. Moreover, different outcomes may emerge when the transition terms from the ignorant class to the spreaders or recovered classes are defined under the true mass-action assumption, where these terms are divided by the total population at each time step [44,45]. Such a formulation could provide additional insights into the behavior of the new ISCR model, particularly when applied to the description of news spreading over a large period of time.

Acknowledgments

The authors are members of the research group GNCS–INdAM. This work has been supported by GNCS–INdAM projects and by the Italian Ministry of University and Research (MUR), through the PRIN 2022 project (CUP: D53C24003350006) *DESTINY* (Stochastic Numerical Modelling For Sustainable Innovation), granted within the framework of the call relating to the scrolling of the final rankings.

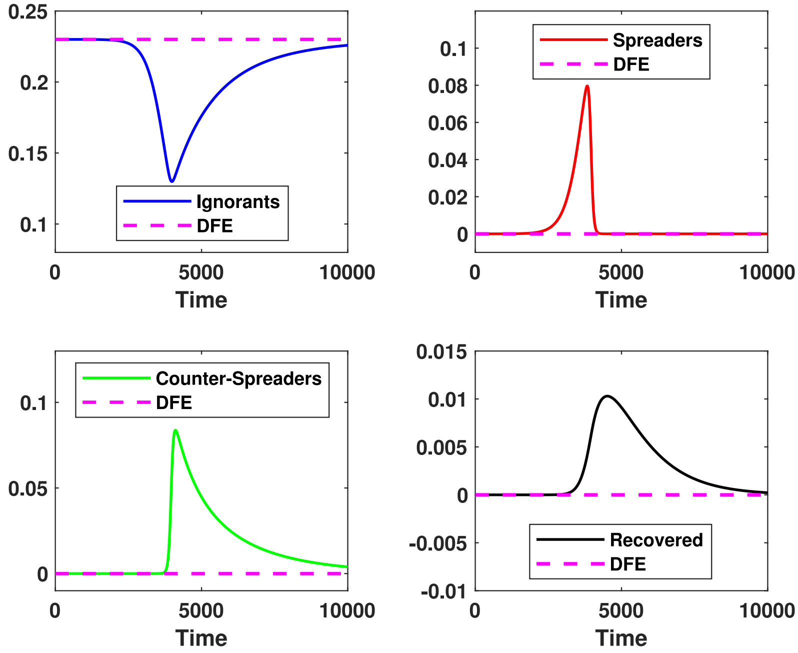

Fig. 7. Numerical solution of the new ISCR with the NSFD method (4.3) for $h = 2$, considering the parameters $\beta = 0.07$, $\alpha = 0.01$, $\gamma = 0.01$, $\mu = 0.01$, $\kappa = 0.06$, $\omega 1 = 1.8406$, $\omega 2 = 0.83151$, $\Lambda = 0.00023$, $\delta = 0.001$, and the initial condition $I_0 = \frac{\Lambda}{\delta}$, $S_0 = C_0 = R_0 = 0.000001$.

Appendix

In Section 3.2, we mentioned the existence of four different types of equilibrium points for the continuous ISCR model (3.1). These points, which correspond also in the discrete case for the NSFD method (4.2) or (4.3), are presented below. They have been computed using the software *Mathematica*, version 14.1.

1. The DFE

$$\{I_{DFE}, S_{DFE}, C_{DFE}, R_{DFE}\} = \left\{\frac{\Lambda}{\delta}, 0, 0, 0\right\}.$$

2. The SPE $\{I_{SPE}, S_{SPE}, 0, R_{SPE}\}$, where

$$I_{SPE} = \frac{1}{2\beta^2\kappa^2}\left(\beta\delta\kappa - \delta\gamma\kappa + r_1\right),$$

$$S_{SPE} = \frac{1}{2\beta\gamma\kappa^2}\left(-\delta(\beta+\gamma)\kappa + r_1\right),$$

$$R_{SPE} = \frac{1}{2\beta^2\delta\gamma\kappa^2}(\beta^2\kappa(\delta^2 + 2\gamma\kappa\Lambda) - \beta\delta r_1 + \delta\gamma(\delta\gamma\kappa - r_1)),$$

with $r_1 = \sqrt{\kappa^2(-2\beta\delta^2\gamma + \delta^2\gamma^2 + \beta^2(\delta^2 + 4\gamma\kappa\Lambda))}$.

3. The CPE $\{I_{CPE}, 0, C_{CPE}, R_{CPE}\}$, where

$$I_{CPE} = \frac{1}{2\alpha^2\kappa^2}(\alpha\delta\kappa - \delta\kappa\mu + r_2),$$

$$C_{CPE} = \frac{1}{2\alpha\mu\kappa^2}\left(-\delta(\alpha+\mu)\kappa + r_2\right),$$

$$R_{CPE} = \frac{1}{2\alpha^2\delta\mu\kappa^2}(\alpha^2\kappa(\delta^2 + 2\mu\kappa\Lambda) - \alpha\delta r_2 + \delta\mu(\delta\mu\kappa - r_2)),$$

with $r_2 = \sqrt{\kappa^2(-2\alpha\delta^2\mu + \delta^2\mu^2 + \alpha^2(\delta^2 + 4\kappa\Lambda\mu))}$.

4. Two different *CE* points, denoted by $CE_i = \{I_{CE_i}, S_{CE_i}, C_{CE_i}, R_{CE_i}\}$, $i = 1, 2$, that, as shown in numerical experiments, in some cases may be not both acceptable or one acceptable and the other not. By setting $u = (\gamma - \mu + \omega_1 - \omega_2)$,

$$\begin{aligned} r_3 = \mathrm{sqrt}\{&(\kappa^2(\alpha^2(4\gamma\kappa\Lambda(\omega_1-\omega_2)+\delta^2 u)+\beta^2(4\kappa\Lambda\mu(\omega_1-\omega_2)+\delta^2 u)+\\ &-2\alpha(\beta(2\kappa\Lambda(\gamma+\mu)(\omega_1-\omega_2)+\delta^2 u)+\delta^2(\omega_1-\omega_2)u)+\\ &+2\beta\delta^2(\omega_1-\omega_2)u+\delta^2(\omega_1-\omega_2)^2 u)u(\alpha\gamma-\beta(\mu-\omega_1+\omega_2))^2)\}, \end{aligned}$$

$$d_1 = \frac{1}{2(\alpha-\beta)(\alpha\gamma-\beta\mu)(\alpha\gamma-\beta(\mu-\omega_1+\omega_2))},$$
$$d_2 = \frac{1}{(\omega_1-\omega_2)u}, \quad o = \omega_1-\omega_2, \quad m_1 = \mu-\omega_1+\omega_2,$$

their expression is as follows.

(a) CE_1 reads

$$\begin{aligned}
I_{CE_1} &= d_1(\alpha^2\delta\gamma\kappa u + \beta^2\delta\kappa u m_1 + \beta\delta\kappa o m_1 u - r_3 - \alpha\delta\kappa u(\gamma o + \beta u)),\\
S_{CE_1} &= d_1 d_2 \, \big(\, \alpha^3\delta\gamma\kappa u(\gamma - o) + \beta\mu(-\beta^2\delta\kappa u m_1 + \beta\delta\kappa o u m_1 - r_3) +\\
&\quad - \alpha^2\delta\kappa u(-\gamma o(\gamma+o) + \beta(\gamma^2 + 2\gamma m_1 - o m_1)) +\\
&\quad + \alpha((\gamma+o)r_3 + \beta\delta\kappa o(\gamma^2(-\mu - m_1) + 2\gamma m_1^2 + o m_1^2) +\\
&\quad + \beta^2\delta\kappa(-\gamma\mu m_1 - m_1^3 + \gamma^2(\mu + m_1)))\,\big),\\
C_{CE_1} &= d_1 d_2(\alpha\gamma - \beta m_1)(-\beta^2\delta\kappa u(\mu+o) + \beta\delta\kappa o u m_1 +\\
&\quad - \alpha^2\delta\gamma\kappa u + \alpha\delta\kappa u(\beta(\gamma+\mu+o) - \gamma o) - r_3),\\
R_{CE_1} &= d_1 d_2 o \, \big(\, \alpha^3\gamma\kappa(\delta^2 + 2\gamma\kappa\Lambda)u - \beta^2\delta^2\kappa(\gamma^2 + \mu^2 + \gamma(-2m_1 + o) +\\
&\quad - 3\mu o + 2o^2)m_1 - \beta^3\kappa(\delta^2 + 2\kappa\Lambda\mu)m_1 u + \delta u r_3 +\\
&\quad + \beta\delta(-\delta\kappa o u^2 m_1 + r_3) - \alpha^2\kappa u(\delta^2\gamma(u+o) +\\
&\quad + \beta(\delta^2(2\gamma + m_1) + 2\gamma\kappa\Lambda(\gamma + \mu + m_1))) +\\
&\quad - \alpha(\beta\delta^2\kappa(-\gamma^3 + \gamma m_1^2 + \gamma^2(m_1 - o) +\\
&\quad - m_1^2(m_1 - o)) + \delta(-\delta\gamma\kappa o u^2 + r_3) +\\
&\quad - \beta^2\kappa u(\delta^2(\gamma + 2m_1) + 2\kappa\Lambda(\mu m_1 + \gamma(\mu + m_2))))\,\big)\,.
\end{aligned}$$

(b) For CE_2, $I_{CE_2} = I_{CE_1}$, and

$$\begin{aligned}
S_{CE_2} &= d_1 d_2 \, \big(\, \alpha^3\delta\gamma\kappa u(\gamma - o) + \beta\mu(-\beta^2\delta\kappa u m_1 + \beta\delta\kappa o u m_1 + r_3) +\\
&\quad - \alpha^2\delta\kappa u(-\gamma o(\gamma+o) + \beta(\gamma^2 + 2\gamma m_1 - o m_1)) +\\
&\quad - \alpha((\gamma+o)r_3 + \beta\delta\kappa o(\gamma^2(\mu - m_1) - 2\gamma m_1^2 - o m_1^2) +\\
&\quad + \beta^2\delta\kappa(\gamma\mu m_1 + m_1^3 - \gamma^2(\mu + m_1)))\,\big),\\
C_{CE_2} &= d_1 d_2(\alpha\gamma - \beta m_1)(-\beta^2\delta\kappa u(\mu+o) + \beta\delta\kappa o u m_1 +\\
&\quad - \alpha^2\delta\gamma\kappa u + \alpha\delta\kappa u(\beta(\gamma+\mu+o) - \gamma o) + r_3),\\
R_{CE_2} &= d_1 d_2 o \, \big(\, \alpha^3\gamma\kappa(\delta^2 + 2\gamma\kappa\Lambda)u - \beta^2\delta^2\kappa(\gamma^2 + \mu^2 + \gamma(-2m_1 + o) +\\
&\quad - 3\mu o + 2o^2)m_1 - \beta^3\kappa(\delta^2 + 2\kappa\Lambda\mu)m_1 u - \delta u r_3 - \beta\delta(\delta\kappa o u^2 m_1 + r_3) +\\
&\quad - \alpha^2\kappa u(\delta^2\gamma(u+o) + \beta(\delta^2(2\gamma + m_1) + 2\gamma\kappa\Lambda(\gamma + \mu + m_1))) +\\
&\quad + \alpha(\beta\delta^2\kappa(\gamma^3 - \gamma m_1^2 - \gamma^2(m_1 - o) + m_1^2(m_1 - o)) +\\
&\quad + \delta(\delta\gamma\kappa o u^2 + r_3) + \beta^2\kappa u(\delta^2(\gamma + 2m_1) +\\
&\quad + 2\kappa\Lambda(\mu m_1 + \gamma(\mu + m_2))))\,\big)\,.
\end{aligned}$$

Data availability

The data that has been used is confidential.

References

[1] M. Casillo, F. Colace, D. Conte, M. De Santo, M. Lombardi, S. Mottola, D. Santaniello, A multi-feature Bayesian approach for fake news detection, CSoNet 2020, in: Computational Data and Social Networks, vol. 9, Springer International Publishing, 2020, pp. 333–344.

[2] G. Giordano, S. Mottola, B. Paternoster, A short review of some mathematical methods to detect fake news, Circuits Systems Signal Process. 14 (2020) 255–265.

[3] A. Cardone, P. Díaz de Alba, B. Paternoster, Influence of age group in the spreading of fake news: contact matrices in social media, in: 16th International Conference SITIS, IEEE, 2022.

[4] A. Cardone, P. Diaz de Alba, B. Paternoster, Analytical properties and numerical preservation of an age-group susceptible-infected-recovered model: Application to the diffusion of information, J. Comput. Nonlinear Dyn. 19 (6) (2024).

[5] M. Castiello, D. Conte, S. Iscaro, Using epidemiological models to predict the spread of information on Twitter, Algorithms 16 (8) (2023) 391.

[6] R. D'Ambrosio, P. Díaz de Alba, G. Giordano, B. Paternoster, A modified seir model: stiffness analysis and application to the diffusion of fake news, in: ICCSA, Springer International Publishing, 2022, pp. 90–103.

[7] R. D'Ambrosio, G. Giordano, S. Mottola, B. Paternoster, Stiffness analysis to predict the spread out of fake information, Futur. Internet 13 (9) (2021) 222.

[8] M.T. Hoang, H.T. Pham, Global dynamics and numerical simulation of a modified epidemiological model for viral marketing on social networks, Math. Comput. Simulation 228 (2025) 225–244.
[9] D. Ignatius, Modeling the Spread of Information on Twitter, (Master's thesis), California State Polytechnic University, Pomona, CA, USA, 2018.
[10] M. Maleki, E. Mead, M. Arani, N. Agarwal, Using an epidemiological model to study the spread of misinformation during the black lives matter movement, 2021, Preprint arXiv:2103.12191.
[11] M. Muhlmeyer, S. Agarwal, Information Spread in a Social Media Age: Modeling and Control, CRC Press, 2021.
[12] M. Muhlmeyer, S. Agarwal, A.J. Huang, Modeling social contagion and information diffusion in complex socio-technical systems, IEEE Syst. J. 14 (4) (2020) 5187–5198.
[13] N.K. Sivaraman, S. Baijal, S.B. Muthiah, On the usage of epidemiological models for information diffusion over twitter, Soc. Netw. Anal. Min. 13 (1) (2023) 133.
[14] H. Wang, F. Wang, K. Xu, Modeling Information Diffusion in Online Social Networks with Partial Differential Equations, vol. 7, Springer Nature, 2020.
[15] Z. Ahmad, G. Bonanomi, A. Cardone, A. Iuorio, G. Toraldo, F. Giannino, Fractal-fractional sirs model for the disease dynamics in both prey and predator with singular and nonsingular kernels, J. Biol. Syst. 32 (4) (2024) 1487–1520.
[16] M. Martcheva, An introduction to mathematical epidemiology, N. Y. Springer 61 (2015) 9–31.
[17] S.M. Treibert, Mathematical Modelling and Nonstandard Schemes for the Corona Virus Pandemic, Springer Spektrum, 2021.
[18] D. Conte, R. D'Ambrosio, G. Giordano, S. Mottola, B. Paternoster, Stiff problems nowadays: Novel numerics and fake news, In AIP Conf. Proc. 2849 (1) (2023) AIP Publishing.
[19] R. D'Ambrosio, Numerical Approximation of Ordinary Differential Problems: From Deterministic To Stochastic Numerical Methods, vol. 148, Springer, 2023, pp. 1–385.
[20] D. Breda, S. De Reggi, R. Vermiglio, A numerical method for the stability analysis of linear age-structured models with nonlocal diffusion, SIAM J. Sci. Comput. 46 (2) (2024) A953–A973.
[21] S. Blanes, A. Iserles, S. Macnamara, Positivity-preserving methods for ordinary differential equations, ESAIM Math. Model. Numer. Anal. 56 (6) (2022) 1843–1870.
[22] I. Higueras, T. Roldán, Strong stability preserving properties of composition Runge–Kutta schemes, J. Sci. Comput. 80 (2) (2019) 784–807.
[23] P. Khakzad, A. Moradi, A. Abdi, G. Hojjati, Strong stability preserving second derivative multistep methods, Numer. Algorithms (2024).
[24] C. Scalone, Positivity preserving stochastic θ-methods for selected SDEs, Appl. Numer. Math. 172 (2022) 351–358.
[25] R. Anguelov, Y. Dumont, J.S. Lubuma, M. Shillor, Dynamically consistent nonstandard finite difference schemes for epidemiological models, J. Comput. Appl. Math. 255 (2014) 161–182.
[26] R. Anguelov, J.M.S. Lubuma, Contributions to the mathematics of the nonstandard finite difference method and applications, Numer. Methods Partial. Differ. Equ. 17 (5) (2001) 518–543.
[27] D. Conte, N. Guarino, G. Pagano, B. Paternoster, Positivity-preserving and elementary stable nonstandard method for a COVID-19 SIR model, Dolomites Res. Notes Approx. 15 (5) (2022) 65–77.
[28] D. Conte, N. Guarino, G. Pagano, B. Paternoster, On the advantages of nonstandard finite difference discretizations for differential problems, Numer. Anal. Appl. 15 (3) (2022) 219–235.
[29] D. Conte, G. Pagano, T. Roldan, High Order Nonstandard Finite-Difference Methods. Submitted.
[30] D. Conte, G. Pagano, B. Paternoster, Nonstandard finite differences numerical methods for a vegetation reaction–diffusion model, J. Comput. Appl. Math. 419 (2023) 114790.
[31] S.M. Garba, A.B. Gumel, A.S. Hassan, J.S. Lubuma, Switching from exact scheme to nonstandard finite difference scheme for linear delay differential equation, Appl. Math. Comput. 258 (2015) 388–403.
[32] K.F. Gurski, A simple construction of nonstandard finite-difference schemes for small nonlinear systems applied to SIR models, Comput. Math. Appl. 66 (11) (2013) 2165–2177.
[33] M.T. Hoang, M. Ehrhardt, A second-order nonstandard finite difference method for a general Rosenzweig–MacArthur predator–prey model, J. Comput. Appl. Math. 444 (2024) 115752.
[34] R.E. Mickens, Calculation of denominator functions for nonstandard finite difference schemes for differential equations satisfying a positivity condition, Numer. Methods Partial. Differ. Equ. 23 (3) (2007) 672–691.
[35] C. Millevoi, D. Pasetto, M. Ferronato, A Physics-informed neural network approach for compartmental epidemiological models, PLoS Comput. Biol. 20 (9) (2024).
[36] D. Breda, S. De Reggi, F. Scarabel, R. Vermiglio, J. Wu, Bivariate collocation for computing R0 in epidemic models with two structures, Comput. Math. Appl. 116 (2022) 15–24.
[37] S. De Reggi, F. Scarabel, R. Vermiglio, Approximating reproduction numbers: a general numerical method for age-structured models, Math. Biosci. Eng. 21 (4) (2024) 5360–5393.
[38] C.D. Pagani, S. Salsa, Analisi Matematica, vol. 2, Zanichelli, 2016.
[39] R.E. Mickens, Nonstandard Finite Difference Models of Differential Equations, World Scientific, 1993.
[40] R.E. Mickens, Dynamic consistency: A fundamental principle for constructing nonstandard finite difference schemes for differential equations, J. Diff. Eq. Appl. 11 (2005) 645–653.
[41] Twitter developer option, 2022, Available online: www.developer.twitter.com. (Accessed on 07 December 2022).
[42] Tweepy documentation, 2022, Available online: https://docs.tweepy.org/en/latest/ (Accessed on 07 December 2022).
[43] Treccani encyclopedia, 2024, www.treccani.it/enciclopedia/eol-amin-mahsa/. (Accessed on 30 December 2024).
[44] C.M. De Jong, O. Diekmann, H. Heesterbeek, How does transmission of infection depend on population size?, in: Epidemic Models: Their Structure and Relation To Data, Cambridge University Press, 1996, pp. 84–94.
[45] H. Inaba, Age-Structured Population Dynamics in Demography and Epidemiology, Springer Singapore, 2017, pp. 1–555.